Inorganic Chemistry

Article

pubs.acs.org/IC

New Family of Lanthanide-Based Inorganic–Organic Hybrid Frameworks: $Ln_2(OH)_4[O_3S(CH_2)_nSO_3]\cdot 2H_2O$ (Ln = La, Ce, Pr, Nd, Sm; n = 3, 4) and Their Derivatives

Jianbo Liang, Renzhi Ma, Yasuo Ebina, Fengxia Geng, and Takayoshi Sasaki*

International Center for Materials Nanoarchitectonics (MANA), National Institute for Materials Science (NIMS), 1-1 Namiki, Tsukuba, Ibaraki 305-0044, Japan

Supporting Information

ABSTRACT: We report the synthesis and structure characterization of a new family of lanthanide-based inorganic–organic hybrid frameworks, $Ln_2(OH)_4[O_3S(CH_2)_nSO_3]\cdot 2H_2O$ (Ln = La, Ce, Pr, Nd, Sm; n = 3, 4), and their oxide derivatives. Highly crystallized samples were synthesized by homogeneous precipitation of Ln^{3+} ions from a solution containing α,ω-organodisulfonate salts promoted by slow hydrolysis of hexamethylenetetramine. The crystal structure solved from powder X-ray diffraction data revealed that this material comprises two-dimensional cationic lanthanide hydroxide $\{[Ln(OH)_2(H_2O)]^+\}_\infty$ layers, which are cross-linked by α,ω-organodisulfonate ligands into a three-dimensional pillared framework. This hybrid framework can be regarded as a derivative of UCl_3-type $Ln(OH)_3$ involving penetration of organic chains into two $\{LnO_9\}$ polyhedra. Substitutional modification of the lanthanide coordination promotes a 2D arrangement of the $\{LnO_9\}$ polyhedra. A new hybrid oxide, $Ln_2O_2[O_3S(CH_2)_nSO_3]$, which is supposed to consist of alternating $\{[Ln_2O_2]^{2+}\}_\infty$ layers and α,ω-organodisulfonate ligands, can be derived from the hydroxide form upon dehydration/dehydroxylation. These hybrid frameworks provide new opportunities to engineer the interlayer chemistry of layered structures and achieve advanced functionalities coupled with the advantages of lanthanide elements.

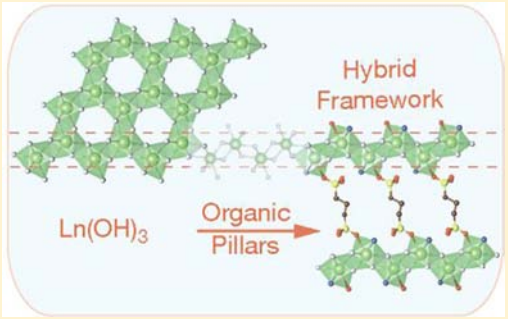

INTRODUCTION

Hybrid materials comprising inorganic and organic components have long been investigated from both fundamental and practical viewpoints. Synergetic combination of these two parts offers a wealth of opportunity for creating enhanced and novel physiochemical properties.[1−6] Design and synthesis of new hybrids, particularly organizing inorganic building blocks and organic ligands into single-crystalline phase, remains a challenging task.[4−6] Major attention is currently focused on metal–organic frameworks (MOFs), well-known porous architectures built by interconnection of metal centers/clusters (0D) and rigid organic linkers.[7−14] Some naturally occurring biocomposites have common structural features, being composed of discrete 2D inorganic building blocks and organic binders. However, synthetic materials mimicking such hybrid structures are rare and have been limited to zeolitic lamellar compounds,[15−17] layered metal phosphates,[18−20] and some examples of metal oxides.[2] Few of these structures are suitable for accommodating lanthanide elements, which is the base of a rich pool of functionalities.[21]

Pillared layered compounds, such as layered metal phosphonates, represent a special three-dimensional framework constructed with polymeric inorganic layers and bridging ligands.[22,23] Interest in pillared inorganic structures stems from the potential for manipulating solid-state functionality and porosity by systematically modifying/designing interlamellar ligands. Evolution of layered zirconium phosphonates, from pure inorganic zirconium phosphates to dense organically pillared frameworks and to microporous intracrystalline composites, demonstrates the concept of crystal engineering.[19,20] Notably, organically pillared compounds are expected to show some new physical phenomena occurring at the interface between the 2D inorganic layers and organic species. Exploration of such aspects is of great interest but largely hindered due to the limited varieties of such hybrid compounds.

Recently, a new series of anion-exchangeable layered host, $Ln_2(OH)_5X\cdot 2H_2O$ (X represents intercalated anions), namely, layered rare-earth hydroxides (LREHs), was discovered.[24−30] Lanthanide ions, in either 8- or 9-fold coordination, are arranged in an ordered manner to produce cationic $\{[Ln_2(OH)_5(H_2O)_2]^+\}_\infty$ layers accommodating a range of charge-balancing anions in between. Flexible anion-exchange ability originating from this structural feature coupled with the attractive physical properties of lanthanide elements can expect potential applications in the field of catalysis, optics, and pharmaceuticals.[28,31,32] The high and variable coordination ability of lanthanides inspires us to design inorganic–organic hybrid structures based on knowledge about the structure and

Received: June 19, 2012
Published: February 7, 2013

   dx.doi.org/10.1021/ic301294j | Inorg. Chem. 2013, 52, 1755−1761

Table 1. Chemical Analysis Results for the Ln−C_3 and Ln−C_4 Samples

chemical formula		elemental analysis (wt %) Ln^{3+}	OH^-	S	C	H_2O
$La_{2.00}(OH)_{4.06}(O_3S(CH_2)_3SO_3)_{1.00}\cdot 2.16H_2O$	obsd	47.30	11.74	11.3	6.12	6.6
	calcd	47.27	11.74	10.9	6.13	6.6
$Pr_{2.00}(OH)_{4.07}(O_3S(CH_2)_3SO_3)_{0.98}\cdot 2.06H_2O$	obsd	48.08	11.75	11.5	6.05	6.3
	calcd	48.09	11.81	10.7	6.02	6.3
$Nd_{2.00}(OH)_{4.08}(O_3S(CH_2)_3SO_3)_{1.00}\cdot 2.14H_2O$	obsd	48.42	11.73	11.3	6.05	6.5
	calcd	48.21	11.51	10.7	6.02	6.4
$Sm_{2.00}(OH)_{4.09}(O_3S(CH_2)_3SO_3)_{1.00}\cdot 2.10H_2O$	obsd	49.47	11.42	11.2	5.90	6.2
	calcd	49.30	11.40	10.5	5.90	6.2
$La_{2.00}(OH)_{3.99}(O_3S(CH_2)_4SO_3)_{0.98}\cdot 1.88H_2O$	obsd	46.87	11.45	11.2	7.90	5.7
	calcd	46.85	11.44	11.9	7.90	6.0
$Pr_{2.00}(OH)_{4.10}(O_3S(CH_2)_4SO_3)_{0.99}\cdot 1.84H_2O$	obsd	46.94	11.59	11.3	7.87	5.5
	calcd	47.09	11.65	10.6	7.94	5.5
$Nd_{2.00}(OH)_{4.06}(O_3S(CH_2)_4SO_3)_{1.07}\cdot 2.04H_2O$	obsd	47.74	11.42	10.9	8.50	6.1
	calcd	46.12	11.04	11.0	8.21	5.9
$Sm_{2.00}(OH)_{4.16}(O_3S(CH_2)_4SO_3)_{1.08}\cdot 2.04H_2O$	obsd	47.74	11.17	10.7	8.24	5.8
	calcd	46.89	11.02	10.8	8.08	5.7

chemistry of $Ln_2(OH)_5X\cdot 2H_2O$.[33] Herein, we report the synthesis and structural characterization of a new series of lanthanide-based inorganic−organic hybrid frameworks, $Ln_2(OH)_4[O_3S(CH_2)_nSO_3]\cdot 2H_2O$ (Ln = La, Ce, Pr, Nd, Sm; n = 3, 4). These compounds adopt a pillared framework built up from cationic hydroxide layers and organic linkers. They are constructed based on engineering of lanthanide coordination and 2D arrangement of $\{LnO_9\}$ polyhedra. Considering the importance of lanthanide elements, this novel structure as well as the photoluminescence properties displayed will enrich the studies on pillared framework compounds.

EXPERIMENTAL SECTION

Materials. Lanthanide nitrates, $Ln(NO_3)_3\cdot xH_2O$ (Ln = La, Ce, Pr, Nd, and Sm, purity of 99.99%) were purchased from Aldrich. Organodisulfonate salts, $Na_2[O_3S(CH_2)_nSO_3]$ (n = 3, 4, purity > 99%), were obtained from Tokyo Chemical Industry (TCI) Co., Ltd. Hexamethylenetetramine (HMT, $C_6H_{12}N_4$, purity > 99.5%) was obtained from Wako Pure Chemical Industry, Ltd. These chemicals were used as received. Milli-Q filtered water (resistivity >18 MΩ·cm) was used throughout.

Synthesis. In a typical synthesis, a homogeneous solution was prepared by dissolving 2.5 mmol of $Ln(NO_3)_3\cdot xH_2O$, 12.5 mmol of organodisulfonate salts, and 0.30 g of HMT in 500 mL of water. This solution was heated and refluxed under nitrogen gas flow to yield a precipitate. In this process, the HMT was progressively decomposed to release ammonia. The slow and controlled increase of the pH value (from 6 to above 11) promoted precipitation of more than 95% of lanthanide ions. The product was recovered by filtration, washed by copious amounts of water, rinsed using ethanol, and finally dried to a constant weight at a controlled humidity of ∼70%.

Chemical Analysis. The content of rare-earth elements was determined by the EDTA-titration method using murexide as an indicator after dissolving the sample with HCl solution. To determine the amount of OH, a weighed amount of sample (about 0.1 g) was first dissolved in 25 mL of 0.1 M HCl standard solution. Then, the residual amount of HCl was determined by NaOH titration (0.1 M standard solution). The contents of sulfur and carbon were determined by element analysis using a LECO CS-412 analyzer. Water content was determined from thermogravimetric analysis (TGA) data.

Characterization. Powder XRD patterns were collected by a Rigaku Rint-2200 diffractometer using a monochromatic Cu Kα radiation (λ = 1.5406 Å). The morphology of the samples was examined by a scanning electron microscope (SEM), Keyence VE8800. Transmission electron micrographs (TEM) and selected area electron diffraction (SAED) patterns were obtained using a JEOL-3100F energy-filtered transmission electron microscope. The specimen for TEM observation was prepared by dispersing the sample in ethanol with sonication followed by drying a few drops on a holey carbon grid. FT-IR spectra were recorded on a Varian 7000e FT-IR spectrophotometer equipped with a liquid-nitrogen-cooled MCT detector using the KBr pellet method. TGA measurements were carried out on a Rigaku TGA-8120 instrument in the temperature range of 25−1000 °C at a heating rate of 5 °C·min^{-1}. Excitation and emission photoluminescence (PL) spectra were obtained at room temperature by means of a Hitachi F-4500 fluorescence spectrometer.

RESULTS AND DISCUSSION

Synthesis and Structure Characterization of $Ln_2(OH)_4[O_3S(CH_2)_nSO_3]\cdot 2H_2O$ (n = 3, 4). Polycrystalline samples were synthesized by a homogeneous precipitation route. Refluxing a solution containing $Ln(NO_3)_3$, disodium salts of α,ω-alkanedisulfonate, and HMT yielded precipitates of well-developed microplatelets (Supporting Information, Figure S1). Monophasic samples could be obtained for elements La, Pr, Nd, and Sm. A minor amount of CeO_2 coexisted in the Ce samples. The compounds are formulated as $Ln_2(OH)_4[O_3S(CH_2)_nSO_3]\cdot 2H_2O$ (n = 3, 4) based on chemical analysis results (Table 1). For simplicity, the sample is abbreviated as Ln−C_n hereafter. The chemical reactions are summarized as

$$C_6H_{12}N_4 + 10H_2O \rightarrow 6HCHO\uparrow + 4NH_4^+ + 4OH^-$$

$$2Ln^{3+} + [O_3S(CH_2)_nSO_3]^{2-} + 4OH^- + 2H_2O \rightarrow Ln_2(OH)_4[O_3S(CH_2)_nSO_3]\cdot 2H_2O\downarrow$$

Powder XRD patterns show that all the Ln−C_3 and Ln−C_4 are isostructurally crystallized in a monoclinic system. The in-plane cell parameters are nearly identical to each other, whereas the basal spacing for the Ln−C_4 compound (14.0 Å) is about 0.9 Å larger than that of the Ln−C_3 sample. Systematic absence of $h + l = 2n + 1$ for $h0l$ and $k = 2n + 1$ for $0k0$ (Supporting Information, Figure S2) suggests the presence of the n-glide plane and a 2_1 screw axis, referring to the space group $P2_1/n$ (No. 14). The crystal structure was first solved from the powder XRD pattern by the direct method using EXPO2009.[34] The resulting model was modified by whole-pattern fitting and

dx.doi.org/10.1021/ic301294j | Inorg. Chem. 2013, 52, 1755−1761

MEM (maximum entropy method) analysis in alternate turns in the Rietan-FP program and finally refined by the Rietveld method.[35,36] The structure is illustrated for La−C_3 as a typical example, as shown in Figure 1 and Table 2.

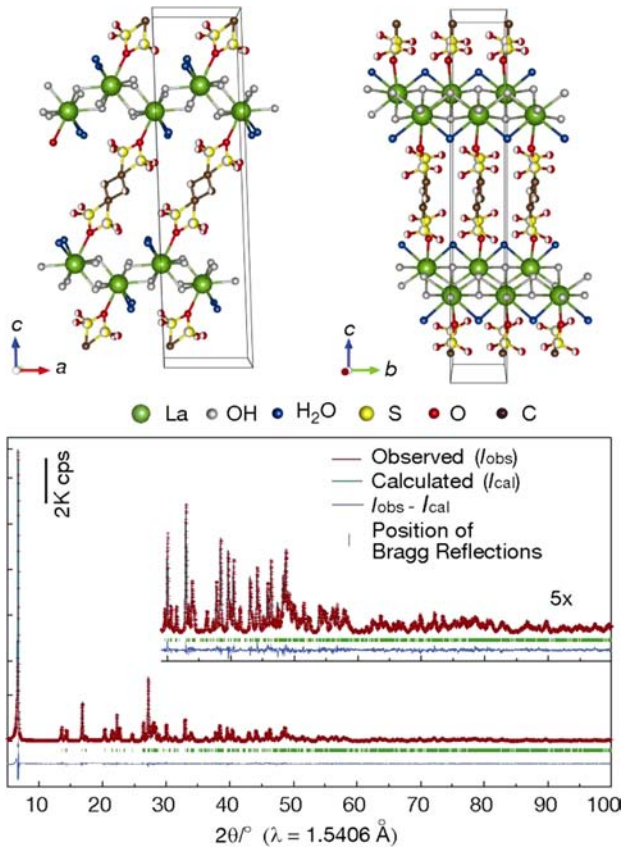

Figure 1. Crystal structure and full Rietveld analysis profile of the La−C_3 compound. Final R factors are R_{wp} = 10.11% (S = 1.11), R_p = 7.42%, R_I = 1.35% and R_F = 0.50%. Half-occupied carbon, sulfur, and oxygen atoms are indicated by the half-filled circles.

Table 2. Structure Parameters of $La_2(OH)_4[O_3S(CH_2)_3SO_3]\cdot 2H_2O$[a]

atom	g	x	y	z	U(Å^2)[b]
La	1.0	0.5085(2)	0.000(2)	0.7825(1)	0.010(1)
OH1	1.0	0.617(1)	0.49(1)	0.2742(2)	0.010(1)
OH2	1.0	0.2652(9)	0.007(9)	0.2905(3)	
H_2O	1.0	0.863(1)	0.00(1)	0.3464(2)	
O1	1.0	0.193(1)	0.550(3)	0.3715(2)	
O2	0.5	0.511(5)	0.185(8)	0.3889(10)	
O3	0.5	0.515(4)	0.785(7)	0.375 (1)	
O4	0.5	0.909(3)	0.195(5)	0.5561(8)	
O5	0.5	0.971(3)	0.779(5)	0.5722(9)	
S1	0.5	0.394(1)	0.484(8)	0.3979(3)	0.029(2)
S2	0.5	0.187(1)	0.49(1)	0.4234(3)	
C1	1.0	0.080(2)	0.96(1)	0.0362(5)	0.027(6)
C2	0.5	0.619(3)	0.53(2)	0.490(1)	

[a]Space group: $P2_1/n$ (No. 14). Lattice parameters: a = 6.4259(1) Å, b = 3.95768(6) Å, c = 26.1502(4) Å, β = 91.932(1)°. [b]A soft constraint, supposing O atoms in OH, H_2O, and SO_3 groups having an identical thermal parameter, is imposed in the refinement; the same strategy is applied to S and C atoms.

This compound can be described as a 3D framework comprising cationic $\{[La(OH)_2(H_2O)]^+\}_\infty$ host layers bridged by α,ω-alkanedisulfonate pillars. The lanthanide ions are 9-fold coordinated, among which six are from OH groups, two from H_2O molecules, and one from a SO_3 group of the organic pillar. The geometry of the $\{LaO_9\}$ polyhedron is a slightly distorted tricapped trigonal prism. Along the b axis, the polyhedra are connected to linear columns by sharing triangular faces, presenting the nearest neighboring La−La distance of 3.96 Å. These columns are then linked into infinite $\{[La(OH)_2(H_2O)]^+\}_\infty$ layers by sharing OH−OH edges. Such linkage produces a quasi-hexagonal arrangement of the polyhedra, giving an La−La distance of 4.10 Å across the columns. This feature can also be observed from the quasi-hexagonal in-plane electron diffraction (ED) pattern (see Supporting Information, Figure S3). In the layers, each OH group links to three lanthanide ions (μ_3-linkage) whereas the H_2O molecule serves as μ_2-connecter. In addition to these OH groups and H_2O molecules, one oxygen atom of the SO_3 group contributes to lanthanide coordination. This monodentate bonding is pointing toward the interlayer region. The corresponding La−O distance of 2.58 Å is close to that for the OH group and H_2O molecule (2.52−2.77 Å). Each α,ω-alkanedisulfonate ion is coordinated to two lanthanide ions from neighboring layers, bridging the lanthanide hydroxide layers into a rigid 3D framework. FT-IR spectra are consistent with these structural features (Supporting Information, Figure S4). In the gallery, the linear alkanedisulfonate ions take two equivalent configurations, and thus, the relevant positions for O and S are split. The alkane chains are nearly parallel to the ac plane but tilted toward the bc plane at an angle of ~38.8°. Slot-like voids are noticed between these alkane chains, which are expected to be hydrophobic.

Further structure analyses reveal that the other Ln−C_3 compounds are isostructurally crystallized in such framework structure. In addition, the Ln−C_4 series, despite consisting of a different α,ω-alkanedisulfonate ligand, adopt a similar framework structure. These pillared layered compounds display a common structure topology, as illustrated in Figure 2. They present a new family of hybrid framework materials where both the inorganic and the organic components can be engineered.

Structure Topology of the Pillared Frameworks. The $\{[La(OH)_2(H_2O)]^+\}_\infty$ host layer described here is built up from $\{LaO_9\}$ polyhedra. The 9-fold La−O coordination is reminiscent of the UCl_3-type $La(OH)_3$, a nonlamellar structure built by closest packing of $\{La(OH)_9\}$ subunits.[37,38] The $\{LaO_9\}$ polyhedra in the pillared structure can be derived from $La(OH)_3$ by substituting one-third of the OH groups with three oxygen atoms, one from the SO_3 group and the other two from H_2O molecules. Note that in both structures the OH group serves as a μ_3-connecter, and the polyhedra are interconnected in an identical manner. The close similarities in La−OH distance and La−OH−La angles, as shown in Figure 3a, suggest that the pillared framework can be regarded as a substitutional derivative of UCl_3-type $La(OH)_3$. A structure topotaxy is revealed from the lattice projections, as depicted in Figure 3b. In UCl_3-type $La(OH)_3$ (hexagonal system, $P6_3/m$), the $\{La(OH)_9\}$ polyhedra is a regular tricapped trigonal prism with 3-fold symmetry. The polyhedra are joined via face sharing into a linear column, and each column is laterally joined with three neighboring ones, extending infinitely in the UCl_3-type tunnel structure. For the pillared framework, incorporating the SO_3 group and H_2O molecules in lanthanide coordination

dx.doi.org/10.1021/ic301294j | Inorg. Chem. 2013, 52, 1755−1761

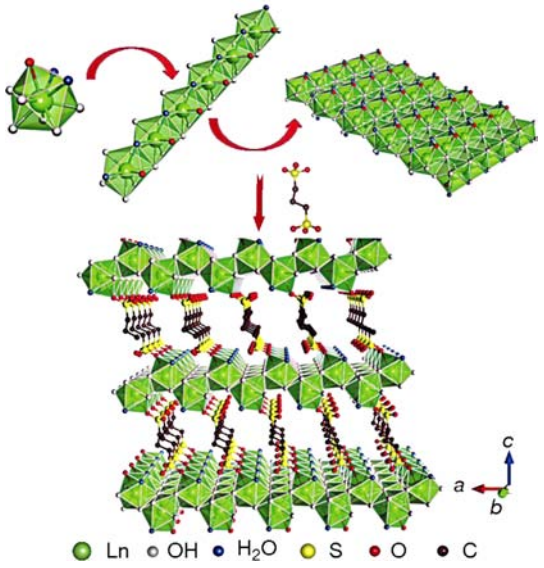

Figure 2. General structure illustration of the pillared layered framework $Ln_2(OH)_4[O_3S(CH_2)_nSO_3]\cdot 2H_2O$. $\{LnO_9\}$ polyhedra and corresponding interconnectivity, from linear column to infinite two-dimensional layer and to three-dimensional pillared framework, are demonstrated.

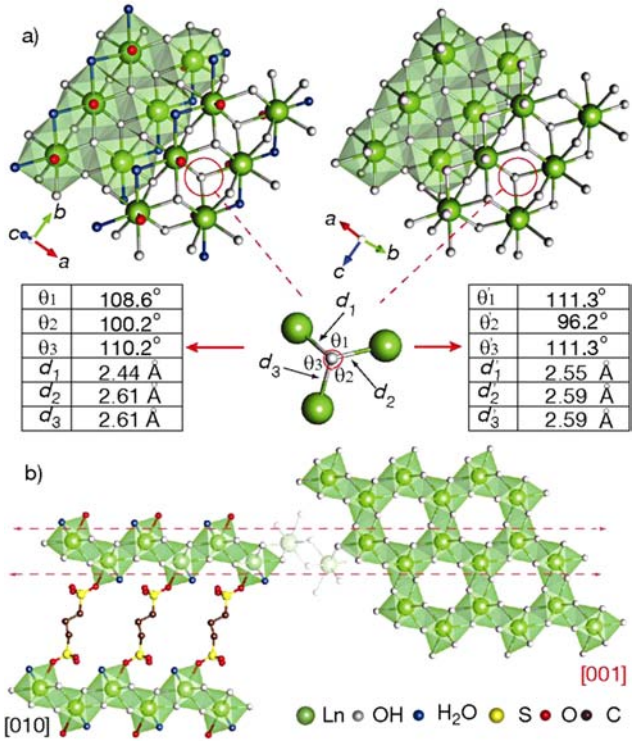

Figure 3. (a) Polyhedra topology and (b) projections of the pillared layered framework (left) and the UCl_3-type $La(OH)_3$ (right). Interatomic distance (d) and La–O–La angle (θ) are listed in panel a. Layer motif is indicated by the red dotted lines in panel b. Topotaxy between these two structures can be understood from the projections.

produces a structural anisotropy. The column can only laterally link to two neighbors, thereby extending in a planar manner to produce the 2D host layer. This topotaxy can be attributed to the nearly identical polyhedra geometry and connectivity between these two structures. Incorporation of organo-disulfonate ligands and water molecules represents the key for 3D to 2D transformation.

In contrast to the pure 9-fold coordination in the pillared framework structure, the layered compounds of $Ln_2(OH)_5X\cdot 2H_2O$ (X = Cl^- and NO_3^-) recently reported are featured by a different structure topology involving the copresence of 8- and 9-fold lanthanide coordination.[25,28,30] In these compounds, the $\{LnO_9\}$ polyhedra are arranged to form a column in the same way as the pillared compound whereas the $\{LnO_8\}$ polyhedra are also linked into a linear chain by sharing edges. The $\{[Ln_2(OH)_5(H_2O)_2]^+\}_\infty$ layer is generated by arranging these columns and chains in alternate sequence, in which the $\{LnO_8\}$ polyhedra can be considered as "nodes" between the $\{LnO_9\}$ columns (see Supporting Information, Figure S5). The $\{LnO_8\}$ nodes connect to the $\{LnO_9\}$ polyhedra via sharing either edges or triangular faces, thereby producing a quasi-hexagonal arrangement of the nearest neighboring lanthanide ions. In such polyhedral arrangement, the in-plane unit-cell dimensions are double those in the present pillared structure. In-plane selected area electron diffraction (SAED) analyses support this structural relationship.[25,30]

Evolution of Framework Oxide Derivatives via Dehydration/Dehydroxylation Reaction. The pillared framework structures can be retained upon heating to 100 °C. Thermogravimetric data (Supporting Information, Figure S6) show that the thermal evolution of the pillared frameworks involves five steps: (I) dehydration, (II) dehydroxylation, (III and IV) cracking of the organic species (sharp weight loss) and oxidization of sulfonate into sulfate (a slow weight gaining process), and (V) release of SO_3 from the solid. The final products are $Ln_2O_2SO_4$, as identified from the XRD data. The chemical reactions are formulated as

$$Ln_2(OH)_4[O_3S(CH_2)_nSO_3]\cdot 2H_2O \rightarrow Ln_2(OH)_4[O_3S(CH_2)_nSO_3] + 2H_2O\uparrow \quad (I)$$

$$Ln_2(OH)_4[O_3S(CH_2)_nSO_3] \rightarrow Ln_2O_2[O_3S(CH_2)_nSO_3] + 2H_2O\uparrow \quad (II)$$

$$Ln_2O_2[O_3S(CH_2)_nSO_3] + ((3n+1)/2)O_2 \rightarrow Ln_2O_2SO_4 + SO_3\uparrow + nCO_2\uparrow + nH_2O\uparrow \quad (III–V)$$

Their thermal behaviors are exemplified in the case of La–C_3, as shown in Figure 4. Dehydration initiated at 120 °C and terminated at about 170 °C with a weight loss of 6.6%, which indicates the loss of 2.2 water molecules per formula weight. The dehydrated product, $La_2(OH)_4[O_3S(CH_2)_3SO_3]$, has lattice parameters of a = 6.4031(7) Å, b = 3.9309(7) Å, c = 24.572(3) Å, and β = 91.277(8)° (Figure 5b). The in-plane lattice parameters a and b are similar to those of the original phase, suggesting a minor change in the lanthanide hydroxide layer upon dehydration. On the other hand, significant interlayer shrinkage took place, which should be due to removal of H_2O molecules and a change in pillar orientation. The second sharp weight loss was observed at the temperature range of 235–275 °C. This event accompanying a weight loss of 5.3% is accounted for by the dehydroxylation reaction, which leads to a hybrid oxide formulated as $La_2O_2[O_3S(CH_2)_3SO_3]$. The sample remained crystalline, and the corresponding XRD pattern (Figure 5c) could be indexed in an orthorhombic system with lattice parameters of a = 8.858(1) Å, b = 4.250(1)

dx.doi.org/10.1021/ic301294j | Inorg. Chem. 2013, 52, 1755–1761

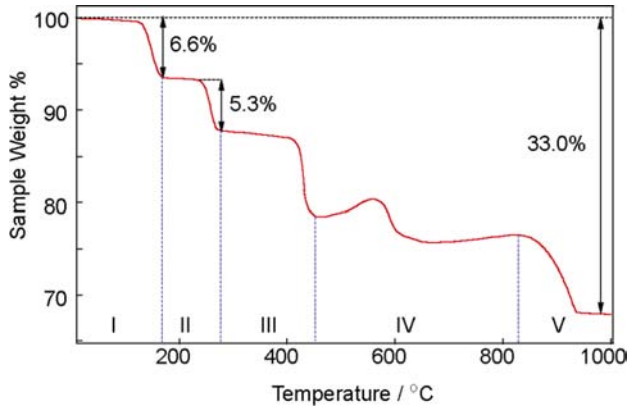

Figure 4. TGA curve of the La−C_3 compound.

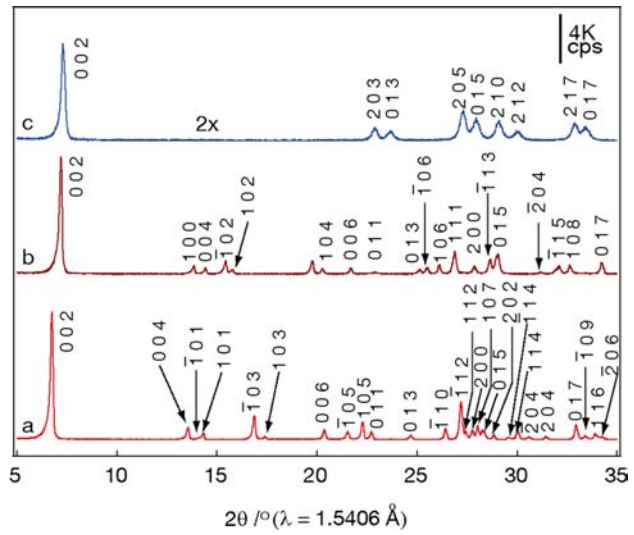

Figure 5. XRD profiles of the La−C_3 sample and the derivatives in the heating process: (a) as-synthesized sample; (b) $La_2(OH)_4[O_3S(CH_2)_3SO_3]$ derived from La−C_3 at 200 °C; (c) $La_2O_2[O_3S(CH_2)_3SO_3]$ derived from La−C_3 at 300 °C.

Å, c = 24.136(4) Å. Note that the in-plane unit cell is close to that of $La_2O_2SO_4$, a layered oxide containing infinite $\{[La_2O_2]^{2+}\}_\infty$ layers.[39] Most likely, $\{[La_2O_2]^{2+}\}_\infty$ layers are comprised in the $La_2O_2[O_3S(CH_2)_3SO_3]$ compound. The basal spacing of 12.1 Å indicates that the α,ω-alkanedisulfonate ligands are sandwiched between the $\{[La_2O_2]^{2+}\}_\infty$ layers, yielding a new pillared oxide framework. On the basis of the structure of $La_2O_2SO_4$ and our XRD data, we propose a structure model for this pillared oxide framework, as illustrated in Figure 6. The gallery height for $La_2O_2[O_3S(CH_2)_3SO_3]$ is estimated as 7.6 Å, considering the thickness of $\{[La_2O_2]^{2+}\}_\infty$ slab, 4.5 Å. Therefore, the tilting of $[O_3S(CH_2)_3SO_3]^{2-}$ ions can be estimated as ~46° (= $\sin^{-1}$ 7.6/10.5). Decomposition of organodisulfonate ions was initiated at 400 °C. Accompanied by the cracking of alkyl chains and oxidization of sulfonate groups, the pillared framework collapsed and finally transformed into $La_2O_2SO_4$ after being heated to 1000 °C. The total weight loss was about 33.0%, close to the theoretical value (30.8%).

Figure 7 shows the FT-IR spectra of the La−C_3 compound, dehydration form, and corresponding pillared oxide. For the La−C_3 compound, the sharp peaks at 3599 and 3506 cm^{-1} are attributable to OH groups free of hydrogen bonding. A broad

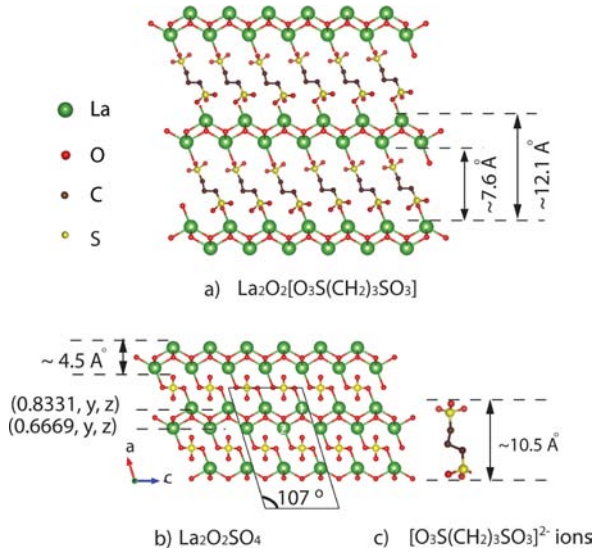

Figure 6. (a) Proposed structure model of $La_2O_2[O_3S(CH_2)_3SO_3]$; (b) crystal structure of $La_2O_2SO_4$. In this compound, the thickness of the $\{[La_2O_2]^{2+}\}_\infty$ layer (d) is determined as $d = a(x_{La1} - x_{La2})\sin\beta + 2r_{La} \approx 4.5$ Å.[39] (c) Illustration of the $[O_3S(CH_2)_3SO_3]^{2-}$ ions. Molecular length is derived from the crystal structure of the La−C_3 compound.

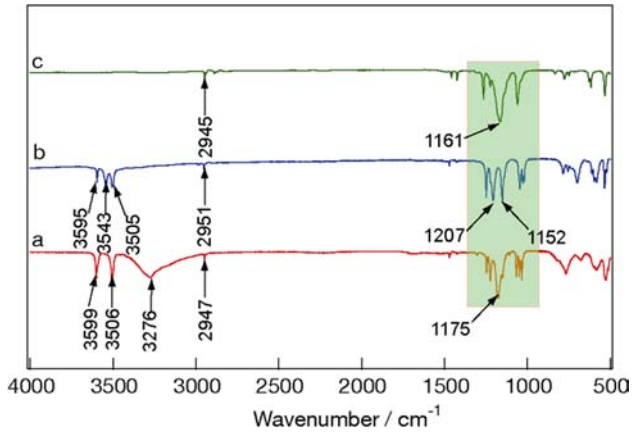

Figure 7. FT-IR spectra for La−C_3 and the derivatives in the heating process: (a) La−C_3 sample; (b) $La_2(OH)_4[O_3S(CH_2)_3SO_3]$ derived from La−C_3 by heating at 200 °C; (c) $La_2O_2[O_3S(CH_2)_3SO_3]$ derived from La−C_3 at 300 °C.

band centered at 3276 cm^{-1} is assigned to O−H stretching modes of water molecules or OH groups associated with hydrogen bonding. After the dehydration reaction, only sharp peaks (at 3595, 3543, and 3505 cm^{-1}) were observed. The absence of the broad band supports complete removal of water molecules. These modes totally disappeared after the sample was treated at 300 °C, supporting transformation to the oxide. For the three samples, the presence of the organic component can be confirmed by the stretching vibration of the CH_2 groups, 2947 cm^{-1} for La−C_3 compound (Figure 7a), 2951 cm^{-1} for the dehydration form (Figure 7b), and the peaks at 2945 cm^{-1} and weak bands in the vicinity for the oxide form. At the same time, the vibration modes from the SO_3 group, as marked in the green region, are split into multiple peaks. The splitting of the modes, being diagnostic of the SO_3 group in lower symmetry, reflects the bonding nature between the SO_3 group and the rare-earth center. The FT-IR data clearly confirm formation of

dx.doi.org/10.1021/ic301294j | Inorg. Chem. 2013, 52, 1755−1761

pillared hybrid frameworks, either in the hydroxide forms or in the oxide form, as we observed from the XRD and TGA data.

Photoluminescence Properties. The $La_2(OH)_4[O_3S(CH_2)_nSO_3]\cdot 2H_2O$ hybrid framework and corresponding pillared oxides can act as host lattice to accommodate various PL centers. This function is exemplified by Eu doping, a widely used approach toward red-emitting phosphors. We introduced 5% of Eu ions into the La−C_3 host based on previous reports on various lanthanide photoluminescent materials as well as our former study on $Eu:Gd_2(OH)_5Cl\cdot nH_2O$ and as derived $Eu:Gd_2O_3$ phosphor.[31] XRD data confirmed formation of the solid−solution sample (Supporting Information, Figure S7). As shown in Figure 8, a broad intense band was observed around

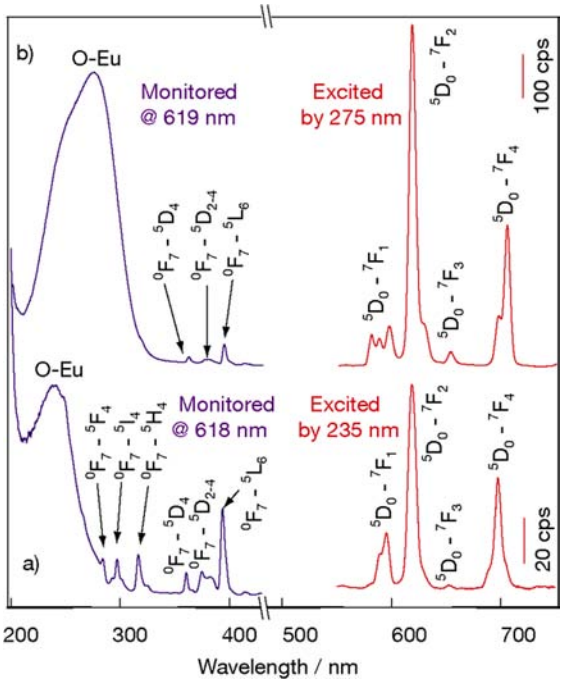

Figure 8. Room-temperature excitation and emission spectra for samples with doping of 5% Eu^{3+} (a) $La_2(OH)_4[O_3S(CH_2)_3SO_3]\cdot 2H_2O$ and (b) $La_2O_2[O_3S(CH_2)_3SO_3]$.

235 nm in the excitation spectrum. This excitation band is similar to that reported for Eu-doped YPO_4, which has been attributed to charge transfer between O^{2-} and Eu^{3+}.[40] A series of sharp lines is ascribable to intra-$4f^6$ transitions within the Eu^{3+} $4f^6$ electronic configurations.[25,31] The emission spectrum consists of typical $^5D_0-{}^7F_J$ (J = 1−4) transitions at 595, 618, 653, and 697 nm, respectively. In particular, the prominent $^5D_0-{}^7F_2$ line (618 nm) showed a sharp peak, which is in contrast to split peaks in the $Eu_2(OH)_5Cl\cdot nH_2O$ compound.[25] Importantly, after conversion to the oxide framework compound, the excitation band was significantly enhanced, as indicated by the intense band around 275 nm in the excitation spectrum. In the corresponding emission spectrum, a sharp $^5D_0-{}^7F_2$ line was observed at 619 nm. This emission line was enhanced eight times in magnitude compared with the hydroxide form, which is due to removal of hydroxyl groups as quenching centers. Another interesting result is the observation of a strong ultraviolet emission centered at 380 nm for a Ce^{3+}-doped sample (Supporting Information, Figure S8), indicating that the present structure can stabilize Ce^{3+}, which is very inclined to be oxidized into Ce^{4+} in alkaline solution and air. These PL data indicate that this new class of hybrid compounds acts as a host of various phosphors, which may invite promising applications toward multifunctional optical materials, for example, oxidative−reduction switches and white-emission optics.[41,42]

CONCLUSIONS

A new series of lanthanide-based inorganic−organic hybrids has been synthesized. This new material is built up from $\{[Ln(OH)_2(H_2O)]^+\}_\infty$ layers inherited from UCl_3-type $Ln(OH)_3$, which are cross-linked by α,ω-alkanedisulfonate ligands into a three-dimensional pillared framework. The topotaxy between the pillared framework and UCl_3-type $Ln(OH)_3$ demonstrates structure engineering from 3D lattice to 2D layer framework based on the similar interconnectivity of the $\{LnO_9\}$ polyhedra. This structure can be obtained with a range of light lanthanide elements and a variety of α,ω-alkanedisulfonate ligands, providing a rich family of pillared frameworks. The size and geometry of the voids within the framework may be tuned depending on the pillars and further engineered by functionalizing the organic pillars with additional functional groups. Some new hybrid structures such as a guest-accessible pillared framework may be further inspired from rational modification of the lanthanide coordination and the polyhedral connectivity. Derivation of hybrid oxides, $Ln_2O_2[O_3S(CH_2)_nSO_3]$, from the organically pillared rare-earth hydroxides enhances the importance of this new class of inorganic−organic hybrids. Multifunctionality coupled with the advantages of lanthanide elements is expected from the pillared frameworks described here, as exemplified by the PL property.

ASSOCIATED CONTENT

Supporting Information

SEM images of the pillared layered rare-earth frameworks, XRD patterns, TEM images, SAED patterns, FT-IR spectra, structure illustration of the $Ln_2(OH)_5X\cdot 2H_2O$ compound, TGA data of the La−C_n samples, XRD pattern and PL spectra of a sample by doping 5% Ce ions into La−C_3 sample. This material is available free of charge via the Internet at http://pubs.acs.org.

AUTHOR INFORMATION

Corresponding Author

*E-mail: sasaki.takayoshi@nims.go.jp.

Notes

The authors declare no competing financial interest.

ACKNOWLEDGMENTS

This work was supported by the World Premier International Center Initiative (WPI Initiative) on Materials Nanoarchitectonics, MEXT, Japan, and CREST of the Japan Science and Technology Agency (JST).

REFERENCES

(1) Guido, K. *Hybrid Materials: Synthesis, Characterization, and Applications*; Wiley-VCH: Weinheim, 2007.
(2) Hagrman, P. J.; Hagrman, D.; Zubieta, J. *Angew. Chem., Int. Ed.* **1999**, *38*, 2638−2684.
(3) Gómez-Romero, P. *Adv. Mater.* **2001**, *13*, 163−174.
(4) Cheetham, A. K.; Rao, C. N. R. *Science* **2007**, *318*, 58−59.
(5) Cheetham, A. K.; Rao, C. N. R.; Feller, R. K. *Chem. Commun.* **2006**, 4780−4795.
(6) Rao, C. N. R.; Cheetham, A. K.; Thirumurugan, A. *J. Phys.: Condens. Matter* **2008**, *20*, 083202.

(7) O'Keeffe, M.; Yaghi, O. M. *Chem. Rev.* **2012**, *112*, 675−702.
(8) Long, J. R.; Yaghi, O. M. *Chem. Soc. Rev.* **2009**, *38*, 1213−1214.
(9) Kitagawa, S.; Kitaura, R.; Noro, S. *Angew. Chem., Int. Ed.* **2004**, *43*, 2334−2375.
(10) Horike, S.; Shimomura, S.; Kitagawa, S. *Nat. Chem.* **2009**, *1*, 695−704.
(11) Yamada, T.; Kitagawa, H. *J. Am. Chem. Soc.* **2009**, *131*, 6312−6313.
(12) Sadakiyo, M.; Yamada, T.; Kitagawa, H. *J. Am. Chem. Soc.* **2009**, *131*, 9906−9907.
(13) Singh, S. K.; Zhang, X. B.; Xu, Q. *J. Am. Chem. Soc.* **2009**, *131*, 9894−9895.
(14) Gu, X. J.; Lu, Z. H.; Jiang, H. L.; Akita, T.; Xu, Q. *J. Am. Chem. Soc.* **2011**, *133*, 11822−11825.
(15) Corma, A.; Díaz, U.; García, T.; Sastre, G.; Velty, A. *J. Am. Chem. Soc.* **2010**, *132*, 15011−15021.
(16) Roth, W. J.; Shvets, O. V.; Shamzhy, M.; Chlubná, P.; Kubů, M.; Nachtigall, P.; Čejka, J. *J. Am. Chem. Soc.* **2011**, *133*, 6130−6133.
(17) Na, K.; Choi, M.; Park, W.; Sakamoto, Y.; Terasaki, O.; Ryoo, R. *J. Am. Chem. Soc.* **2010**, *132*, 4169−4177.
(18) Vivani, R.; Costantino, F.; Taddei, M.About Zirconium Phosphonates. In *Metal Phosphonate Chemistry: From Synthesis to Application*; Chapter 2, RSC: Oxford, 2011.
(19) Gary, B. H. Luminescent Metal Phosphonate Materials. In *Metal Phosphonate Chemistry: From Synthesis to Application*; Chapter 16, RSC: Oxford, 2011.
(20) Alberti, G.; Casciola, M.; Costantino, U.; Vivani, R. *Adv. Mater.* **1996**, *8*, 291−303.
(21) Mao, J. *Coord. Chem. Rev.* **2007**, *251*, 1493−1520.
(22) Clearfield, A.; Kuchenmeister, M. Pillared Layered Materials. In *Supramolecular Architecture*; ACS Symposium Series 499; American Chemical Society: Washington, DC, 1992.
(23) Pergher, S. B. C.; Corma, A.; Fornes, V. *Quím. Nova* **1999**, *22*, 693−709.
(24) Geng, F.; Ma, R.; Sasaki, T. *Acc. Chem. Res.* **2010**, *43*, 1177−1185.
(25) Geng, F.; Xin, H.; Matsushita, Y.; Ma, R.; Tanaka, M.; Izumi, F.; Iyi, N.; Sasaki, T. *Chem.− Eur. J.* **2008**, *14*, 9255−9260.
(26) Geng, F.; Matsushita, Y.; Ma, R.; Xin, H.; Tanaka, M.; Izumi, F.; Iyi, N.; Sasaki, T. *J. Am. Chem. Soc.* **2008**, *130*, 16344−16350.
(27) Geng, F.; Matsushita, Y.; Ma, R.; Xin, H.; Tanaka, M.; Iyi, N.; Sasaki, T. *Inorg. Chem.* **2009**, *48*, 6724−6730.
(28) Gándara, F.; Perles, J.; Snejko, N.; Iglesias, M.; Gómez-Lor, B.; Gutiérrez-Puebla, E.; Monge, M. A. *Angew. Chem., Int. Ed.* **2006**, *45*, 7998−8001.
(29) McIntyre, L. J.; Jackson, L. K.; Fogg, A. M. *Chem. Mater.* **2008**, *20*, 335−340.
(30) Poudret, L.; Prior, T. J.; McIntyre, L. J.; Fogg, A. M. *Chem. Mater.* **2008**, *20*, 7447−7453.
(31) Hu, L.; Ma, R.; Ozawa, T. C.; Sasaki, T. *Angew. Chem., Int. Ed.* **2009**, *48*, 3846−3849.
(32) Lee, B. -I.; Lee, K. S.; Lee, J. H.; Lee, I. S.; Byeon, S. -H. *Dalton Trans.* **2009**, 2490−2495.
(33) Liang, J.; Ma, R.; Geng, F.; Ebina, Y.; Sasaki, T. *Chem. Mater.* **2010**, *22*, 6001−6007.
(34) Altomare, A.; Camalli, M.; Cuocci, C.; Giacovazzo, C.; Moliterni, A. G. G.; Rizzi, R. *J. Appl. Crystallogr.* **2009**, *42*, 1197−1202.
(35) Izumi, F. *J. Ceram. Soc. Jpn.* **2003**, *111*, 617−623.
(36) Izumi, F.; Ikeda, T. *Mater. Sci. Forum* **2000**, *321*−*324*, 198−203.
(37) Zachariasen, W. H. *Acta Crystallogr.* **1948**, *1*, 265−268.
(38) Meyer, G.; Masselmann, S. *Chem. Mater.* **1998**, *10*, 2994−3004.
(39) Zhukov, S.; Yatsenko, A.; Chernyshev, V.; Trunov, V.; Tserkovnaya, E.; Antson, O.; Hölsä, J.; Baulés, P.; Schenk, H. *Mater. Res. Bull.* **1997**, *32*, 43−50.
(40) van Pieterson, L.; Reid, M. F.; Wegh, R. T.; Soverna, S.; Meijerink, A. *Phys. Rev. B* **2002**, *65*, 045113.
(41) Li, Q.; Yam, V. W. *Angew. Chem., Int. Ed.* **2007**, *46*, 3486−3489.
(42) Dang, S.; Zhang, J. H.; Sun, Z. M. *J. Mater. Chem.* **2012**, *22*, 8868−8873.